The Microstructure and Rheology of Mixed Cationic/Anionic Wormlike Micelles

Beth A. Schubert, Eric W. Kaler,* and Norman J. Wagner

Center for Molecular and Engineering Thermodynamics, Department of Chemical Engineering, University of Delaware, Newark, Delaware 19716

Received September 30, 2002. In Final Form: March 12, 2003

The rheology, flow birefringence, and small-angle neutron scattering of mixed cationic/anionic wormlike micellar solutions composed of cetyl trimethylammonium tosylate (CTAT) and sodium dodecyl benzyl sulfonate (SDBS) are studied over a broad range of solution compositions. This combination of experimental techniques enables independent determination of the microstructural length scales (persistence, entanglement, interaction, and contour) that govern the rheological properties. Comparison and contrast of the effect of a hydrotropic salt (NaTosylate) with that of a screening electrolyte (NaCl) demonstrates the influence of micellar charge on the persistence length and, hence, the microstructure and rheology. Surfactant concentration and composition and electrolyte concentration and composition systematically affect the self-assembled microstructure such that a transition in rheological behavior from nonionic wormlike micelles to polyelectrolytes can be spanned.

Introduction

Wormlike micelles have been actively studied in part as models for solutions of linear polymers and polyelectrolytes[1] and recently for applications ranging from drag reduction[2] to oil field fluids[3] and as templates for material synthesis.[4,5] Unlike chemical polymers, self-assembled wormlike micelles can break and re-form under shear, making them stable in applications where high shear rates may be encountered. Under appropriate conditions, the reversible self-assembly of wormlike micelles results in nearly Maxwellian rheological behavior,[6−9] a discovery that generated significant interest from both academic and application perspectives. This "simple" rheology provides a robust method for tailoring product rheological properties without the use of polymers or other additives;[10] however, a detailed understanding of the dependence of the rheological parameters on solution composition is required to tune the material properties for specific applications.

Connecting the chemical composition of the solution to the macroscopic material properties, i.e., structure−property relations, requires knowledge of the self-assembled structure of the solution, which can range in dimension from nanometers to micrometers. The overall contour length, persistence length, and diameter of the micelles are relevant features setting micellar flexibility and mobility. Long-range electrostatic interactions may also play a role in determining micellar interactions and, hence, the rheology, so the Debye screening length and Gouy−Chapman length scales are also potentially important. For concentrated solutions of wormlike micelles, the "mesh size" or distance between entanglements is an additional relevant length scale, as it sets the high-frequency elastic modulus. An illustration with typical values for length scales is shown in Figure 1. The unique rheological properties of wormlike micellar solutions also depend on the time scales or lifetime of these microstructures. For example, because these systems are self-assembled, the rate of stress relaxation is partly controlled by the micellar breakage time and partly by the rate of reptation.[7] All of this information needs to be correlated with the macroscopic rheology to develop structure−property relations.

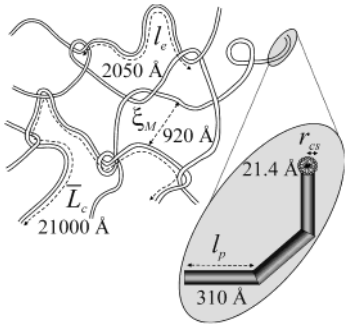

Figure 1. Schematic of wormlike micelles with relevant length scales: contour length, $\bar{L}_c$, entanglement length, l_e, mesh size, ξ_M, persistence length, l_p, and cross-sectional radius, r_{cs}. Values shown are those measured for a solution with 1.5% total surfactant at a CTAT/SDBS ratio of 97/3 with 0.10% added NaTosylate.

Previous study has focused primarily on nonionic micellar systems, for which a detailed theory has been developed to link macroscopic rheology to the mesoscopic system properties.[6−9] Investigations of ionic[11−15] and mixed cationic/anionic systems[16,17] demonstrate significant de-

* Corresponding author: kaler@che.udel.edu.

(1) Magid, L. J. *J. Phys. Chem. B* **1998**, *102*, 4064−4074.
(2) Zakin, J. L.; Bewersdorff, H. W. *Rev. Chem. Eng.* **1998**, *14*, 253−320.
(3) Maitland, G. C. *Curr. Opin. Colloid Interface Sci.* **2000**, *5*, 301−311.
(4) Kim, W. J.; Yang, S. M. *Chem. Mater.* **2000**, *12*, 3227−3235.
(5) Kline, S. R. *Langmuir* **1999**, *15*, 2726−2732.
(6) Granek, R.; Cates, M. E. *J. Chem. Phys.* **1992**, *96*, 4758−4767.
(7) Cates, M. E.; Candau, S. J. *J. Phys.: Condes. Matter* **1990**, *2*, 6869−6892.
(8) Cates, M. E. *J. Phys.: Condes. Matter* **1996**, *8*, 9167−9176.
(9) Cates, M. E. *Macromolecules* **1987**, *20*, 2289−2296.
(10) Rose, G. D.; Teot, A. S. In *Structure and Flow in Surfactant Solutions*; ACS Symposium Series 578; American Chemical Society: Washington, DC, 1994; pp 352−369.
(11) Kern, F.; Lequeux, F.; Zana, R.; Candau, S. J. *Langmuir* **1994**, *10*, 1714−1723.
(12) Soltero, J. F. A.; Puig, J. E.; Manero, O. *Langmuir* **1996**, *12*, 2654−2662.
(13) Oda, R.; Narayanan, J.; Hassan, P. A.; Manohar, C.; Salkar, R. A.; Kern, F.; Candau, S. J. *Langmuir* **1998**, *14*, 4364−4372.

10.1021/la020821c CCC: $25.00
Published on Web 04/18/2003

viations from the simple picture developed for nonionic systems, and these differences have of course been attributed to electrostatic effects, such as counterion screening, salt penetration, and electrostatic interactions. However, a quantifiable and definitive elucidation of the influence of electrostatic interactions on wormlike micelle rheology and solution microstructure is lacking.

In this study we explore cationic/anionic surfactant mixtures as model, wormlike micelles with electrostatic interactions. Although significantly more complicated in behavior than nonionics, the use of these mixed charged micelles provides additional control over the various mesoscopic structural properties through variations in the chemical composition. For example, the micellar surface charge density, and hence the micelle contour length and persistence length, can be directly manipulated by changing the ratio of anionic to cationic surfactant. The addition of electrolytes can screen intermicellar interactions as well as affect micellar persistence length and, in the case of a hydrotropic salt, also reduce the micellar charge through direct incorporation into the micelle. Consequently, the influence of both a simple electrolyte and a hydrotropic salt on wormlike micelle structure and rheology is reported below. Examining such an extensive parameter space enables the development of a data set that yields a more complete picture of mixed cationic/anionic wormlike micelle behavior. The combination of rheology, rheo-optics, and small-angle neutron scattering (SANS) provides a powerful method to *quantify* the various length and time scales, thus providing all of the relevant mesoscale parameters that link chemical composition to rheology. The results are useful for the practical formulation of cationic/anionic mixed micelle solutions and provide an extensive database for subsequent modeling.

Theory

Wormlike micelles can self-assemble in aqueous solutions of cationic surfactants with or without added salt, but wormlike micelles are usually made by adding strongly binding counterions such as salicylate[15,18] or tosylate,[12] and they commonly form in cationic/anionic surfactant mixtures,[16,19] where the oppositely charged surfactant can be thought of as an extremely strong hydrotrope.[17] In dilute solution, the preferred self-assembled geometry may be spherical micelles, but as surfactant concentration increases, it often becomes more energetically favorable for micelles to grow axially into rodlike micelles. The linear growth of these micelles can eventually result in overall contour lengths ($\bar{L}_c$) of micrometers. A mean-field treatment[7] of this growth process for neutral or highly screened micelles yields a prediction for the average contour length of the wormlike micelle in terms of the surfactant concentration, c, the scission energy required to form two hemispherical endcaps, E_c, temperature, T, and Boltzmann's constant, k_B, as:

$$\bar{L}_c \sim c^{1/2} \exp[E_c/k_B T] \tag{1}$$

For charged micelles in the absence of salt, the scission energy has an additional electrostatic component, E_e, due to the repulsion of the charges along the backbone that favors shorter cylinders. In this case, the mean micelle size in the semidilute regime is given by:[20]

$$\bar{L}_c \sim \phi^{1/2} \exp\left[\frac{1}{2k_B T}(E_c - E_e)\right] \tag{2}$$

where the electrostatic contribution E_e is

$$E_e \cong k_B T l_B r_{cs} v^2 \phi^{1/2} \tag{3}$$

Here, l_B is the Bjerrum length, r_{cs} is the radius of the cylindrical micelle, v is the effective charge per unit length, and ϕ is the micellar volume fraction. At higher ϕ, micellar growth is characterized by a power law, $\bar{L}_c \propto \phi^{1/2(1+\Delta)}$, where Δ is related to the endcap charge and depends logarithmically on volume fraction.[20]

The linear viscoelastic rheology of *nonionic* wormlike micellar solutions has been shown to be approximately Maxwellian, exhibiting a single, dominant relaxation time. This is a direct consequence of the self-assembled nature of a micelle, because in addition to the usual reptation motion exhibited by linear polymers in melts or concentrated solutions, micelles can also break and re-form to relieve stress. Breakage is assumed to be a unimolecular scission process with a rate constant k_1, having units of per unit arc length per unit time. The time required for a micelle to break, τ_{break}, is then related to the average contour length by:[9]

$$\tau_{break} = \frac{1}{k_1 \bar{L}_c} \tag{4}$$

Cates and co-workers showed that in the "fast breaking" limit, i.e., when breakage occurs rapidly in comparison to the time required for reptation, τ_{rep}, the convolution of reptation and micelle breakage leads to Maxwellian behavior with a single relaxation time τ_R given by:[7]

$$\tau_R = (\tau_{break}\tau_{rep})^{1/2} \tag{5}$$

For Maxwell fluids, the elastic and viscous moduli G' and G'' vary with frequency as:

$$G'(\omega) = \frac{G'_\infty \omega^2 {\tau_R}^2}{1 + \omega^2 {\tau_R}^2}$$

$$G''(\omega) = \frac{G'_\infty \omega \tau_R}{1 + \omega^2 {\tau_R}^2} \tag{6}$$

Consequently, the dynamic rheology can be parametrized by the high-frequency plateau modulus, G'_∞, and the relaxation time, τ_R, which is given for a Maxwell fluid as the inverse of the crossover frequency of G' and G''.

Under steady shear flow, wormlike micelles exhibit a low-shear Newtonian plateau, followed by strong shear thinning above a critical shear rate, $\dot{\gamma}_c$. The inverse of this critical shear rate also gives an estimate of the longest micellar structural relaxation time. The Newtonian

(14) Ali, A. A.; Makhloufi, R. *Colloid Polym. Sci.* **1999**, *277*, 270−275.
(15) Hoffmann, H. In *Structure and Flow in Surfactant Solutions*; ACS Symposium Series 578; American Chemical Society: Washington, DC, 1994; pp 2−31.
(16) Koehler, R. D.; Raghavan, S. R.; Kaler, E. W. *J. Phys. Chem. B* **2000**, *104*, 11035−11044.
(17) Raghavan, S. R.; Fritz, G.; Kaler, E. W. *Langmuir* **2002**, *18*, 3797−3803.
(18) Shikata, T.; Hirata, H.; Kotaka, T. *Langmuir* **1987**, *3*, 1081−1086.
(19) Kaler, E. W.; Herrington, K. L.; Murthy, A. K.; Zasadzinski, J. A. N. *J. Phys. Chem.* **1992**, *96*, 6698−6707.
(20) Mackintosh, F. C.; Safran, S. A.; Pincus, P. A. *Europhys. Lett.* **1990**, *12*, 697−702.

plateau is characterized by a zero-shear viscosity, η_o, defined for a Maxwell fluid as

$$\eta_o = G'_\infty \tau_R \tag{7}$$

For nonionic wormlike micellar solutions at fixed temperature, the only controllable parameter for a given chemistry is the surfactant concentration, c. Cates and co-workers have developed scaling laws specific to nonionic systems for the concentration dependence of the high-frequency modulus, linear viscoelastic relaxation time, and zero-shear viscosity, as follows:

$$G'_\infty \sim \phi^{9/4} \quad \text{or} \quad G'_\infty \sim c^{9/4} \tag{8}$$

$$\tau_R \sim c^{5/4} \tag{9}$$

$$\eta_o \sim c^{7/2} \tag{10}$$

While these predictions have also been quantitatively verified for the ionic $CpC_{16}PyCl/NaSal$ system in NaCl,[21] numerous deviations for other ionic systems have been discovered experimentally. If electrostatic interactions are significant, the exponent for the elastic modulus is greater than 9/4.[11] Steeper power law dependencies of the zero-shear viscosity have been observed,[22,23] as well as maxima as a function of surfactant concentration.[11−15] Maxima in η_o as a function of added electrolyte have also been reported,[15,24,25] often explained by the onset of (hypothesized) micellar branching. Further investigation and at least partial resolution of these issues are outlined below.

Micellar Length Scales. The rheological properties depend on the mesoscale structure of the micellar solution, so the appropriate length scales must be quantified. A combination of rheology, rheo-optics, and SANS methods is used to determine the micellar physical properties as follows.

As τ_{break}/τ_{rep} increases, deviations from Maxwellian behavior are observed at high frequency. As the Rouse or "breathing" modes become important, the viscous modulus may go through a minimum, G''_{min}, at higher frequencies, such as observed for concentrated polymer solutions. The location of this minimum provides a relationship between the contour length and entanglement length,[6] l_e:

$$G''_{min}/G'_\infty \approx l_e/L_c \tag{11}$$

The entanglement length, an estimate of the average distance between entanglement points along the wormlike micelle, can be calculated from the persistence length, l_p, and mesh size:[26,27]

$$l_e \approx \xi_M^{5/3}/l_p^{2/3} \tag{12}$$

Rubber elasticity theory relates the plateau in the elastic modulus to the mesh size,[26,27] ξ_M, by:

$$\xi_M \approx (k_B T/G'_\infty)^{1/3} \tag{13}$$

The persistence length, l_p, provides an estimate of micellar flexibility. While wormlike micelles can be extremely long and flexible with contour lengths on the order of micrometers, on small length scales of order l_p, they act as rigid rods. Techniques such as light or neutron scattering or flow birefringence allow l_p to be measured. A "bending rod" or Holtzer plot representation of light or small angle neutron scattering data enables a qualitative determination of both the persistence length and contour length.[28,29] Application of Pedersen and Schurtenburger's calculation of the form factor for a wormlike chain with excluded volume interactions[30] allows extraction of values of both the persistence length and the contour length from a least-squares fitting of the scattering spectra in the absence of significant intermicellar interactions. However, this theory currently can only be applied to dilute solutions.

The persistence length can also be calculated from the stress-optical coefficient. The stress optic rule postulates that the stress tensor and refractive index tensor are linearly related by the stress optic coefficient, C. In component form, the magitude of the birefringence, $\Delta n'$, and sine or cosine of the orientation angle, χ, can be related to the shear stress, σ_{xy}, or first normal stress difference, N_1, respectively, through the stress optic coefficient:

$$\Delta n' \sin(2\chi) = 2C\sigma_{xy} \qquad \Delta n' \cos(2\chi) = CN_1 \tag{14}$$

The stress optic rule holds for polymeric solutions[31] as well as wormlike micellar solutions.[32,33] A plot of $\Delta n' \sin(2\chi)$ versus shear stress should be linear with a slope equal to twice the stress optic coefficient. The cosine component can be used to verify the value of C against normal stress data; however, if data for N_1 are unavailable, Laun's rule:

$$\left(\frac{G'}{\omega^2}\right)_{\omega\to 0} = \left(\frac{N_1}{2\dot{\gamma}^2}\right)_{\dot{\gamma}\to 0} \tag{15}$$

can be combined with the stress optic rule to allow comparison of the dynamic rheological data to optical measurements.[34]

Interpretation of the stress optic coefficient to obtain structural information, such as the micellar persistence length, requires a model. For a flexible chain, the stress optic coefficient is:[35]

$$C = \frac{2\pi(n^2+2)^2\Delta\alpha}{45nk_B T} \tag{16}$$

Here, n is the refractive index of the solvent and $\Delta\alpha$ the anisotropy in polarizability of one Kuhn segment. The polarizability can then be related to the persistence length by using the structural model proposed by Shikata:[32]

(21) Berret, J. F.; Appell, J.; Porte, G. *Langmuir* **1993**, *9*, 2851−2854.
(22) Cappelaere, E.; Cressely, R.; Decruppe, J. P. *Colloid Surf., A* **1995**, *104*, 353−374.
(23) Hassan, P. A.; Raghavan, S. R.; Kaler, E. W. *Langmuir* **2002**, *18*, 2543−2548.
(24) Candau, S. J.; Khatory, A.; Lequeux, F.; Kern, F. *J. Phys. IV* **1993**, *3*, 197−209.
(25) Rehage, H.; Hoffmann, H. *Mol. Phys.* **1991**, *74*, 933−973.
(26) Gennes, P. G. d. *Scaling concepts in polymer physics*; Cornell University Press: Ithaca, NY, 1979.
(27) Doi, M., Edwards, S. F. *The Theory of Polymer Dynamics*; Clarendon Press: Oxford, 1986.
(28) Schmidt, M.; Paradossi, G.; Burchard, W. *Makromol. Chem., Rapid Commun.* **1985**, *6*, 767−772.
(29) Magid, L. J.; Han, Z.; Li, Z.; Butler, P. D. *Langmuir* **2000**, *16*, 149−156.
(30) Pedersen, J. S.; Laso, M.; Schurtenberger, P. *Phys. Rev. E* **1996**, *54*, R5917−R5920.
(31) Janeschitz-Kriegl, H. *Polymer Melt Rheology and Flow Birefringence*; Springer-Verlag: Berlin, 1983.
(32) Shikata, T.; Dahman, S. J.; Pearson, D. S. *Langmuir* **1994**, *10*, 3470−3476.
(33) Humbert, C.; Decruppe, J. P. *Colloid Polym. Sci.* **1998**, *276*, 160−168.
(34) Laun, H. M. *J. Rheol.* **1986**, *30*, 459−501.
(35) Kuhn, W. G., F. *Z. Kolloid* **1942**, *28*, 248.

$$\Delta\alpha = 2\Delta\alpha^{\circ} l_p/\lambda \quad (17)$$

This model assumes each Kuhn segment consists of several surfactant disklike monomers of width λ, with $\Delta\alpha^{\circ}$ being the difference in polarizability between the radial and axial directions of the segment.

For ionic micelles, the persistence length l_p, which characterizes the flexibility of the wormlike micellar chain, bears some analogy to that of a polyelectrolyte chain,[1] so that the total persistence length is given by the sum of the intrinsic persistence length, l_p°, and an electrostatic contribution, l_p^{e}: $l_p = l_p^{\circ} + l_p^{e}$. The electrostatic persistence length depends both on micellar charge and on the Debye length, κ^{-1}. The Odijk−Skolnick−Fixman (OSF) theory[36,37] predicts l_p^{e} should depend on the Debye length and L_o, the mean distance between charged groups, as:

$$l_p^{\circ} = (l_B/4)(\kappa^{-1}/L_o)^2 \quad (18)$$

The major assumptions of OSF theory are that the polyelectrolyte is locally stiff and that excluded volume interactions are not significant. Experimental data[38,39] for polyelectrolytes as well as results from Monte Carlo simulations of wormlike micelles with high surface charge density at low ionic strength[40,41] support l_p^{e} scaling with κ^{-2}. Recent variational calculations[42] indicate that the scaling of l_p^{e} with the Debye length is more complex than the OSF prediction and depends on the relative value of the intrinsic persistence length, l_p°, to l_B/L_o^2.

Finally, SANS measurements at q values beyond any interaction peaks can be analyzed to obtain the micellar cross-sectional radius, r_{cs}, by using a Guinier approximation for the form factor:

$$qI(q) \sim \exp\left(-\frac{1}{2} q^2 R_{g,cs}^2\right) \quad (19)$$

The cross-sectional radius of gyration of the micelles, $R_{g,cs}$, is related to the micellar cross-sectional radius by:

$$r_{cs} = 2^{1/2} R_{g,cs} \quad (20)$$

In summary, measurements of the rheology, rheo-optics, and SANS can, in principle, completely quantify four of the length scales discussed previously—namely, the contour length, mesh size, persistence length, and the micelle diameter. However, the range of data accessible in the laboratory is not always sufficient to determine all properties across broad ranges of composition. Particular caution is needed if micellar branching is possible. The electrostatic length scales can be calculated from the solution chemistry, but complications arise due to charge neutralization in the mixed catanionic systems and with counterion association and penetration into the micelle. In principle, SANS can also provide a quantitative measure of the micellar interactions, but there is as of yet no robust model to enable unambiguous extraction of the micellar interactions from SANS spectra from charged micelles.

Materials and Methods

Cetyl trimethylammonium tosylate (CTAT) was obtained from Sigma and recrystallized three times from a 50/50 mixture of ethanol/acetone. Soft-type (linear chain) sodium dodecyl benzenesulfonate (SDBS) was used as received from TCI. Sodium tosylate was obtained from Sigma-Aldrich and was dried in an oven for 24 h before using. Sodium chloride was used as received from Fisher Scientific. Surfactant solutions were prepared in distilled−deionized water for rheology and in D_2O, purchased from Cambridge Isotopes, for SANS experiments. All work was performed in the single phase region previously characterized.[19]

Rheological measurements were performed using a Rheometric Scientific SR 500 stress-controlled rheometer at 25 ± 0.1 °C. A couette geometry was used with a 32 mm diameter cup and a bob of 29.5 mm × 44.5 mm. The shear rheology was verified to be independent of instrument and tool geometry by comparing measurements for selected samples using a Rheometric Scientific ARES with parallel plate geometry.

SANS measurements were made using the NG-3 spectrometer at the National Institute of Standards and Technology (NIST) in Gaithersburg, MD. The neutron wavelength, λ, was 6 Å with a wavelength spread of $\Delta\lambda/\lambda = 15\%$. The scattering vector, q, ranged from 0.0038 to 0.47 Å^{-1}. Samples were held in 2 mm quartz cells in a temperature-controlled bath at 35 ± 0.1 °C to avoid crystallization in the D_2O solvent. Raw data were corrected for background, detector efficiency, and empty cell scattering and placed on an absolute scale using standards supplied by NIST.

Flow birefringence measurements were made using a Rheometrics Optical Analyzer (ROA)[43] at 25 °C equipped with a double-walled couette geometry (inner cylinder radius of 1.5 cm and a gap of 0.1 cm). A He−Ne laser with a wavelength of 6382 Å propagates down the vorticity direction of the couette cell with an optical path length of 1.57 cm.

Results

In the following results, the surfactant solutions are maintained in the one-phase region of the phase diagram where wormlike micelles are thought to be the self-assembled microstructure.[19] For direct comparison and contrast, the total surfactant concentration is varied first, holding the added salt concentration fixed. Two different added salts, one hydrotropic or "penetrating" (sodium tosylate, which is also the common salt of both surfactants) and one "simple" salt (NaCl) are then explored. Electrostatic screening effects are evident, so the next series varies the added salt concentration at fixed surfactant concentration. Finally, because comparison of salts suggests hydrotrope penetration affects both the micellar charge and length scales, the surfactant ratio is also varied.

Rheology. *Surfactant Concentration.* Previous measurements of CTAT/SDBS micellar solutions with a weight ratio of 97/3 and no added electrolyte demonstrated that the zero-shear viscosity and relaxation time exhibited an anomalous maximum with varying surfactant concentration.[16] This was previously postulated to be a consequence of a maximum in contour length due to a balance between the micellar growth and variations in the electrostatic screening as the counterion concentration increases with the surfactant concentration. The effect of surfactant concentration on the steady shear rheology is shown in Figure 2 for a fixed CTAT/SDBS ratio of 97/3 and an added concentration of sodium tosylate, the hydrotropic salt, of 0.25 wt % (13 mM). The molar ratio of added salt to the total surfactant concentration, C_S/C_D, ranges from 2.3 at

(36) Skolnick, J.; Fixman, M. *Macromolecules* **1977**, *10*, 944−948.
(37) Odijk, T. *J. Polym. Sci., Part B: Polym. Phys.* **1977**, *15*, 477−483.
(38) Mattoussi, H.; Odonohue, S.; Karasz, F. E. *Macromolecules* **1992**, *25*, 743−749.
(39) Maret, G.; Weill, G. *Biopolymers* **1983**, *22*, 2727−2744.
(40) Cannavacciuolo, L.; Pedersen, J. S.; Schurtenberger, P. *J. Phys.: Condens. Matter* **2002**, *14*, 2283−2295.
(41) Cannavacciuolo, L.; Pedersen, J. S.; Schurtenberger, P. *Langmuir* **2002**, *18*, 2922−2932.
(42) Ha, B. Y.; Thirumala, D. *J. Chem. Phys.* **1999**, *110*, 7533−7541.
(43) Fuller, G. G. *Optical Rheometry of Complex Fluids*; Oxford University Press: New York, 1995.

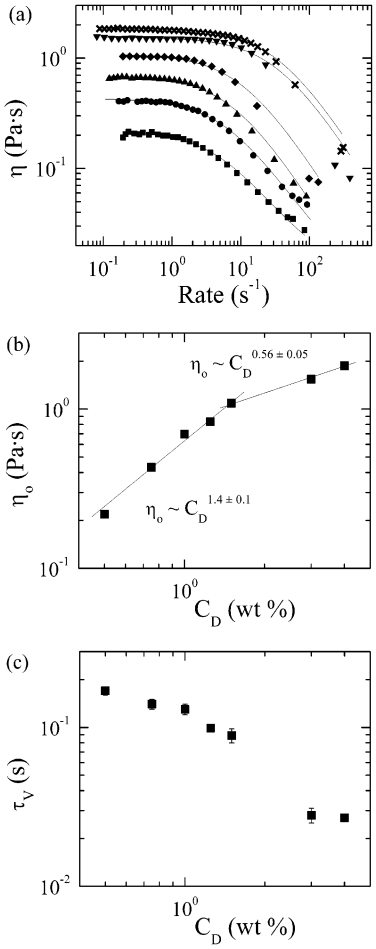

Figure 2. (a) Steady rheological behavior for surfactant concentrations of 0.5% (■), 0.75% (●), 1.0% (▲), 1.5% (◆), 3.0% (▼), and 4.0% (×). Added sodium tosylate concentration is held constant at 0.25%, and CTAT/SDBS ratio is fixed at 97/3. The lines are fits to the data by the Cross model (eq 21), the parameters from which, namely, the zero-shear viscosity, η_o, and shear relaxation time, τ_v, are shown versus surfactant concentration in (b) and (c), respectively. Error bars, if not shown, are the size of the symbols.

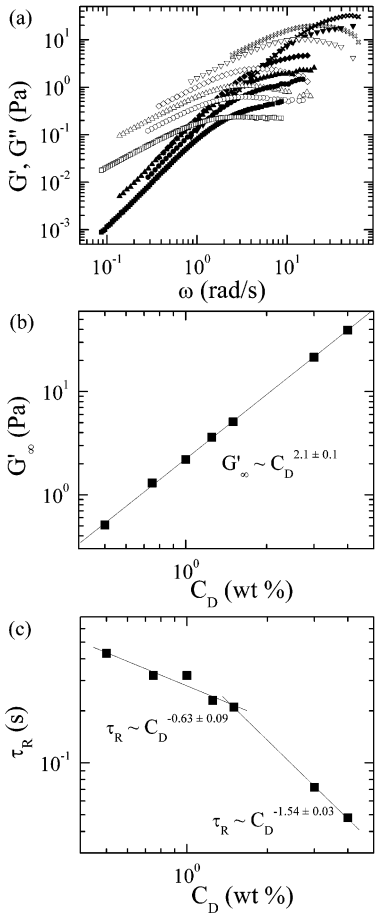

Figure 3. (a) G' (filled symbols) and G'' (open symbols) as a function of frequency in the linear viscoelastic regime. Surfactant concentration by weight is varied from 0.5% (■), 0.75% (●), 1.0% (▲), 1.5% (◆), 3.0% (▼), and 4.0% (×). Added sodium tosylate concentration is held constant at 0.25 wt %, and CTAT/SDBS weight ratio is fixed at 97/3. The dynamic rheology can be parametrized by the high-frequency plateau, G'_∞, and the dynamic relaxation time, $\tau_R = 1/\omega_c$, displayed versus surfactant concentration in (b) and (c), respectively.

the lowest surfactant concentration to 0.15 at the highest value of C_D. All samples show a low shear Newtonian plateau, followed by shear thinning at higher shear rates, characteristic of wormlike micelles. These data are fit by the Cross model[44] to obtain the zero-shear viscosity and an estimation of the shear relaxation time, τ_v

$$\eta(\dot{\gamma}) = \eta_\infty + \frac{\eta_o - \eta_\infty}{1 + (\dot{\gamma}\tau_v)^m} \qquad (21)$$

Here, η_∞ is the high shear viscosity and the exponent m is found to be in the range 0.9−1.0.

The addition of sodium tosylate eliminates the maxima in both zero-shear viscosity and relaxation time reported previously for CTAT/SDBS wormlike micelles without added salt.[16] Although the rheological properties are monotonic functions of the surfactant concentration, the behavior still does not follow that predicted for nonionic micelles. The zero-shear viscosity increases with surfactant concentration (Figure 2b), while the relaxation time *decreases* (Figure 2c), which is also typical of polyelectrolyte solutions.[45,46] The zero-shear viscosity scales with total surfactant concentration as $C_D^{1.4\pm0.1}$ below total surfactant concentrations of 1.5%, and as $C_D^{0.56\pm0.05}$ at concentrations between 1.5 and 4.0 wt % (34−93 mM). This break point of 1.5% total surfactant concentration is physically meaningful, as will be demonstrated in the following.

The linear viscoelastic rheology for these solutions is shown in Figure 3. As surfactant concentration increases, the frequency response becomes more Maxwellian. The plateau modulus increases with concentration as $C_D^{2.1\pm0.1}$, consistent with the scaling predicted for nonionic micelles (Figure 3b). As this is primarily a geometric effect, i.e., for entangled polymers $G'_\infty = \rho_e k_B T$ with ρ_e the entanglement density, the result suggests that increasing concentration in the semidilute regime (at fixed composition and added salt) does not radically alter the wormlike micellar structure. Interestingly, in agreement with the nonlinear rheology, the relaxation time *decreases* as $C_D^{-0.63\pm0.09}$ for surfactant concentrations between 0.5 and 1.5 wt % (11−34 mM) and as $C_D^{-1.5\pm0.1}$ for surfactant concentrations greater than 1.5% (Figure 3c). In summary, the presence of sodium tosylate in CTAT/SDBS wormlike micelles is

(44) Cross, M. M. *J. Colloid Sci.* **1965**, *20*, 417−437.

(45) Krause, W. E.; Tan, J. S.; Colby, R. H. *J. Polym. Sci., Part B: Polym. Phys.* **1999**, *37*, 3429−3437.

(46) Boris, D. C.; Colby, R. H. *Macromolecules* **1998**, *31*, 5746−5755.

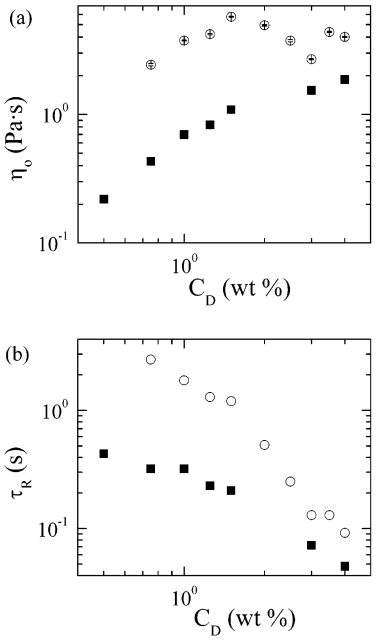

Figure 4. (a) Zero-shear viscosity from steady shear rheology and (b) relaxation time from dynamic rheology, $\tau_R = 1/\omega_c$, as functions of surfactant concentration at a CTAT/SDBS ratio of 97/3 and fixed salt concentration of 0.25% NaTosylate (■) or 0.25% NaCl (○).

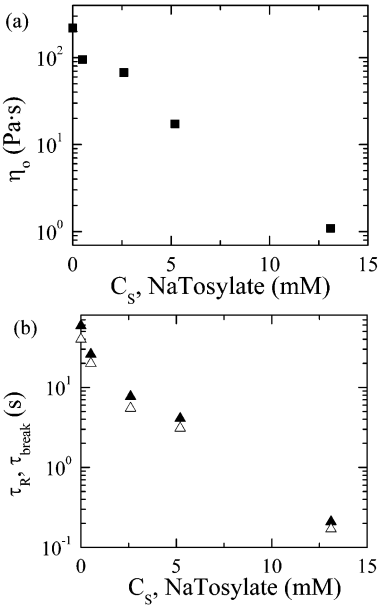

Figure 5. Rheological parameters as a function of added NaTosylate concentration at CTAT/SDBS ratio of 97/3 and fixed surfactant concentration of 1.5%: (a) zero-shear viscosity and (b) relaxation time (▲) and breakage time (△) from dynamic rheology as a function of added NaTosylate concentration at CTAT/SDBS ratio of 97/3 and fixed surfactant concentration of 1.5%.

effective in reducing the influence of electrostatic intermicellar interaction and/or electrostatic contributions to the persistence length, yet it is not sufficient to induce rheological behavior expected for nonionic micelles at the concentrations investigated.

Master rheological curves (Figures S1 and S2 in Supporting Information) were created from all measurements, subsets of which are shown in Figures 2 and 3, to search for significant deviations in the rheological behavior as a function of solution chemistry. The ability to create master curves provides evidence that there are no qualitative changes in the underlying microstructure over the parameter space studied in this work. However, the deviations present at high frequency in the dynamic rheology and at the transition to shear-thinning behavior in the steady rheology indicate there are differences in micellar length and time scales as a function of solution chemistry. The rheology will be parametrized by zero-shear viscosities, relaxation times, and plateau moduli as functions of solution chemistry for comparison and elucidation of the nature of these differences.

To explore further the effect of surfactant concentration on the rheology, 0.25 wt % (44 mM) of the simple electrolyte (a screening salt), NaCl, was added to solutions with a constant CTAT/SDBS ratio of 97/3. The zero-shear viscosity (Figure 4a) goes through a maximum with C_D at approximately 1.5 wt % (34 mM), then decreases until concentration reaches approximately 3% (69 mM), and then increases again. This nonmonotonic behavior is seen in the system without added salt.[16] The maximum in η_o at 1.5% surfactant occurs at approximately at a molar ratio of $C_S/C_D \approx 1$, suggesting electrostatic interactions are the source of the viscosity maximum. For comparison, the zero-shear viscosities for solutions with an equal weight of added NaTosylate increase steadily with C_D (Figure 4a).

As in the case of added sodium tosylate, the relaxation times for solutions with NaCl monotonically decrease with surfactant concentration (Figure 4b), although they are much longer. The relaxation time decreases as $C_D^{-1.2\pm0.2}$ for surfactant concentrations between 0.75 and 1.5% and as $C_D^{-2.6\pm0.2}$ for surfactant concentrations greater than 1.5%. Although the molarity of NaCl (44 mM) is higher than that of NaTosylate (13 mM), the addition of the hydrotropic salt reduces the viscosity and relaxation time significantly more than the screening salt. This is probably due in part to the additional reduction in micellar charge by the tosylate ion, which partitions into the micelle. However, as with the added NaTosylate, the plateau modulus for solutions with added NaCl scales as $C_D^{2.3\pm0.1}$ (see Supporting Information), which is consistent with the model for nonionic wormlike micelles and further confirms that no significant changes in topology are occurring with added NaCl.

Salt Concentration. As evidenced by the comparison of CTAT/SDBS wormlike micelles with and without added salt, added electrolyte can substantially reduce micellar solution viscosities in the concentration ranges investigated. The effect of ionic strength on the rheology was studied further by varying the amount of added sodium tosylate while keeping surfactant concentration and surfactant ratio fixed at 1.5% and 97/3, respectively. Both the zero-shear viscosity (Figure 5a) and relaxation time (Figure 5b) decrease by over 2 orders of magnitude when only 0.25% (13 mM) NaTosylate is added to CTAT/SDBS, corresponding to an increase of the molar ratio C_S/C_D from 0 to 0.4. The plateau modulus remains constant over all salt concentrations studied, so adding salt does not change the mesh size.

The addition of the hydrotropic salt NaTosylate screens the electrostatic interactions and also reduces the micellar surface charge due to penetration of the tosylate ion. The decreases in both η_o and τ_R are approximately linear on a semilog scale, suggesting that micellar breakage is an activated process with an activation energy that scales linearly with the tosylate concentration. Indeed, the micellar breakage time, which can be estimated either from the dynamic rheology as the inverse of the frequency of deviation from Maxwellian behavior (Figure S2) or by

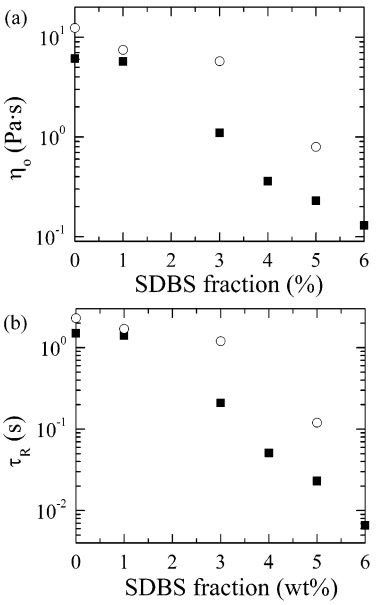

Figure 6. Zero-shear viscosity as a function of SDBS fraction at 1.5% total surfactant and 0.25% NaTosylate (■) or 0.25% NaCl (○).

the method outlined in ref 47, decreases as tosylate is added, confirming that the rheological behavior is controlled by micellar scission.

Surfactant Ratio. The final compositional variable explored was the effect of the ratio of CTAT to SDBS at fixed total surfactant concentration of 1.5% and fixed added electrolyte of 0.25%, where both NaCl and NaTos were investigated. The comparison of penetrating and screening salts suggests that variation in micellar charge density has the greatest influence on the rheology and varying surfactant ratio is the most direct method to vary the net micellar charge density. The zero-shear viscosity decreases as SDBS is added to CTAT in the presence of either salt (Figure 6a), as does the relaxation time (Figure 6b). As the amount of SDBS relative to CTAT increases (i.e., the net micellar charge density decreases), the relaxation time also monotonically decreases. Interestingly, in the presence of NaTosylate, the decrease in relaxation time with added SDBS is nearly exponential except at low concentrations, which suggests that addition of either tosylate or SDBS yields similar reductions in micellar charge. The behavior in the presence of NaCl is less dramatic at the concentrations examined. The plateau modulus (see Supporting Information) remains constant as a function of SDBS fraction in the presence of both electrolytes, as is expected at a constant surfactant concentration. As shown, the addition of either NaCl or NaTosylate eliminates the maxima in viscosity and relaxation time seen in the case of no added salt.[16] Sodium tosylate, the penetrating salt, reduces both the zero-shear viscosity and relaxation time more than sodium chloride, despite NaCl being present at a higher molarity than NaTosylate. As seen in the previous section, the addition of NaTosylate has a similar effect on the rheological parameters, and hence less SDBS is needed to effect an equivalent change in rheology in the presence of NaTosylate as compared to NaCl.

Flow Birefringence. A direct measure of the persistence length with variation in salt concentration is necessary to verify the mechanism by which electrostatic

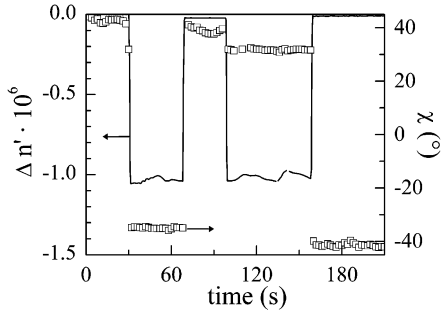

Figure 7. Time-dependent behavior of birefringence, $\Delta n'$ (—), and extinction angle, χ(□), at a shear rate of 3 s^{-1} for a CTAT/SDBS ratio of 95/5 and total surfactant concentration of 1.5 wt % in 0.25 wt % NaCl.

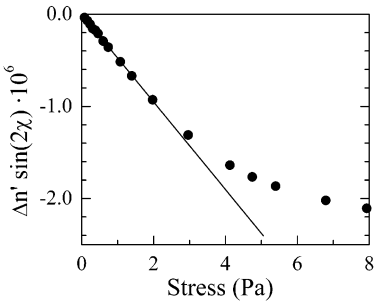

Figure 8. Determination of stress optic coefficient for a CTAT/SDBS ratio of 95/5 and total surfactant concentration of 1.5 wt % in 0.25 wt % NaCl. The line is a fit to the data at low stress.

interactions and screening affect the rheological properties. This is extracted from the stress optic coefficient as follows. Typical time-dependent flow birefringence data are shown in Figure 7 at a shear rate of 3 s^{-1} for a CTAT/SDBS ratio of 95/5 and total surfactant concentration of 1.5% in 0.25% NaCl. During the initial rest zone (0−30 s), the birefringence, $\Delta n'$, starts at zero and the orientation angle, χ, at 45°. At the inception of shear from 30 to 70 s, the birefringence quickly reaches a steady value of -1.0×10^{-6} during shear, and the orientation angle reaches an average value of 35°, relative to the flow direction. Upon cessation of shear from 70 to 100 s, $\Delta n'$ and χ quickly relax back to their rest values. Reversing the flow from 100 to 160 s results in a sign change for χ, although the average values of $\Delta n'$ and χ remain the same. Note that this sample has a rheological relaxation time of ∼0.12 s (Figure 6b) and thus, for the data sampling rate employed, no relaxation or start-up transients can be detected.

The product $\Delta n' \sin(2\chi)$ is plotted against the shear stress for a range of shear rates in Figure 8. Steady-state experimental values of $\Delta n'$ and χ are used, while the stress is obtained from the Cross model fits to the measured shear viscosity. As shown, the stress optic rule is valid until a stress of approximately 2 Pa, after which $\Delta n' \sin(2\chi)$ becomes nonlinear. A stress optic coefficient of $C = -2.4 \times 10^{-7}$ Pa^{-1} is obtained by a fit to the linear portion of the data in Figure 8 (eq 14). This value of C is verified for accuracy by comparing the cosine component to the first normal stress difference, N_1 (Figure S3 in Supporting Information).

The stress optic coefficient can be related to the persistence length using a model of a freely jointed chain (eqs 16 and 17).[32] Once a value of the l_p is known, the entanglement length can be determined from eq 12, where the mesh size is calculated from the plateau modulus in eq 13. This combination of rheology and flow birefringence

(47) Kern, F.; Lemarechal, P.; Candau, S. J.; Cates, M. E. *Langmuir* **1992**, *8*, 437−440.

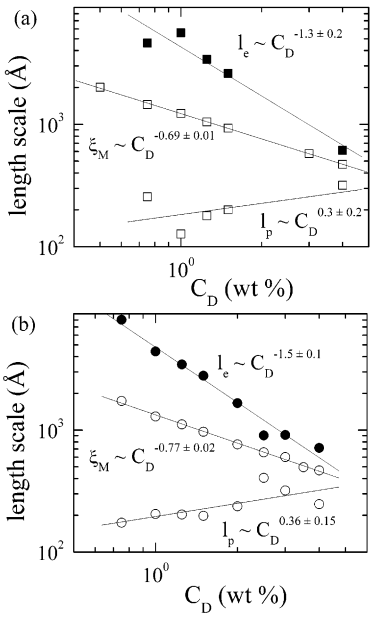

Figure 9. Length scales as a function of surfactant concentration for CTAT/SDBS ratio = 97/3, in 0.25% NaTosylate (a) or 0.25% NaCl (b). Persistence length is shown by gray symbols, mesh size by open symbols, and entanglement length by black symbols.

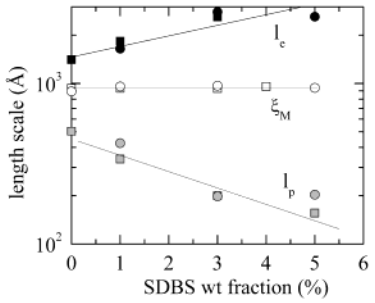

Figure 10. Length scales as a function of SDBS fraction for surfactant concentration of 1.5%, in 0.25% NaTosylate (squares) or 0.25% NaCl (circles). Persistence length is shown by gray symbols, mesh size by open symbols, and entanglement length by black symbols.

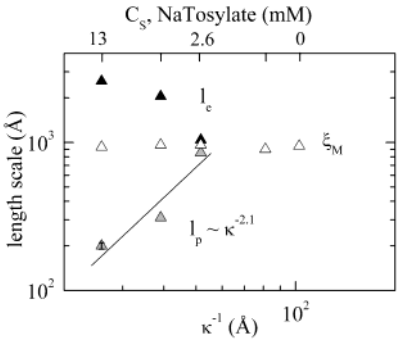

Figure 11. Length scales as a function of Debye length for a fixed CTAT/SDBS ratio of 97/3 and surfactant concentration of 1.5%. The concentration of added NaTosylate varies from zero to 0.25% (13 mM), from right to left, respectively. Persistence length is shown by gray symbols, mesh size by open symbols, and entanglement length by black symbols.

was used to determine these three micellar length scales as functions of the solution chemistry.

First the effect of varying surfactant concentration is explored with added NaTosylate (Figure 9a) and NaCl (Figure 9b). For solutions with added NaTosylate, l_p weakly increases as surfactant concentration increases, while the mesh size and entanglement length decrease as $\xi_M \sim C_D^{-0.69\pm0.01}$ and $l_e \sim C_D^{-1.3\pm0.2}$. The increase in persistence length with surfactant concentration has been observed for other ionic wormlike micellar solutions with added salt, where the persistence length was extracted from fits to measured SANS spectra.[48] In that case, the dependence of l_p on C_D was attributed to interchain interactions. In this work, solutions with added NaCl exhibit scalings of $\xi_M \sim C_D^{-0.77\pm0.02}$ and $l_e \sim C_D^{-1.5\pm0.1}$. The persistence length weakly increases with C_D up to a surfactant concentration of 2.5%, after which it perhaps begins to decrease. In the case of solutions with added NaCl, l_p becomes comparable to both the mesh size, ξ_M, and the entanglement length at surfactant concentrations greater than 2.5%, at which point l_p begins to decrease again. This also corresponds to the point at which the zero-shear viscosity begins to oscillate with surfactant concentration (Figure 4a).

Next, l_p was measured as a function of surfactant ratio at a fixed surfactant concentration of 1.5% and added electrolyte of 0.25%, with both NaCl and NaTosylate being investigated (Figure 10). The persistence length systematically decreases with the addition of SDBS, in agreement with expectation from OSF theory. The mesh size remains constant, which is expected for a fixed surfactant concentration, so the entanglement length increases slightly. As SDBS is added to CTAT, the surface charge density is lowered, thereby increasing L_o, the distance between charges, which decreases the electrostatic contribution to the persistence length (eq 18). This is qualitatively consistent with the measured rheology since an increase in flexibility should result in both a lower zero-shear viscosity and shorter relaxation time.

Finally, the effect of added NaTosylate on the persistence length is studied at a fixed surfactant concentration of 1.5% and a CTAT/SDBS ratio of 97/3 (Figure 11). At a NaTosylate concentration of 0.25%, the persistence length is 200 Å. As the salt concentration decreases, the persistence length increases, eventually reaching 850 Å at 0.05% NaTosylate. Calculating the Debye screening length for these solutions indicates $l_p \sim \kappa^{-2.1\pm0.1}$ (Figure 11) as predicted by eq 18. The mesh size remains constant while the entanglement length increases with added salt. This trend is consistent with the observed rheology because an increase in flexibility with added salt is expected to lower the zero-shear viscosity and relaxation time.

Small Angle Neutron Scattering (SANS). The electrostatic intermicellar interactions influence the rheology of catanionic wormlike micellar solutions. This is demonstrated by comparing the nonmonotonic behavior of the viscosity (Figure 4a) with increasing surfactant concentration with the monotonic increase in measured persistence length (Figure 9). The viscosity falls at concentrations above 1.5 wt % surfactant despite the increase in persistence length, which increases despite the increasing ionic strength. Consequently, the rheology under these conditions must be reflecting intermicellar interactions. To investigate this further, static SANS spectra were measured for samples with varying concentrations of added NaTosylate (Figure 12). The scattering curves are typical for solutions of wormlike micelles, and a strong interaction peak is evident in the spectra for both zero and 0.01% added sodium tosylate. As more salt is added, the electrostatic intermicellar repulsion is screened

(48) Sommer, C.; Pedersen, J. S.; Egelhaaf, S. U.; Cannavacciuolo, L.; Kohlbrecher, J.; Schurtenberger, P. *Langmuir* **2002**, *18*, 2495−2505.

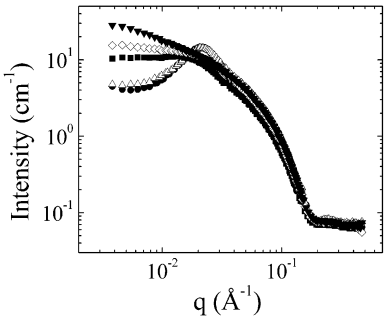

Figure 12. SANS study of effect of varying NaTosylate. CTAT/SDBS ratio is held constant at 97/3 and surfactant concentration is 1.5%. A strong interaction peak is present at zero (●) and 0.01% (△) added NaTosylate. The peak diminishes at 0.05% (■) added salt, with no peak present at 0.10% (◇) and 0.25% (▼) added salt. All spectra overlap is at high q, indicating that the local rodlike geometry is maintained at all salt concentrations.

and the peak disappears. The SANS spectra overlap at larger q values, indicating the local rodlike geometry is maintained at all salt concentrations. This high-q region allows determination of the micellar cross-sectional radius (eqs 19 and 20), which remains relatively unaffected by the addition of NaTosylate, ranging from 21.2 to 21.6 Å over the range of salt concentrations studied.

A "bending rod" plot, which displays the scattering data in the form $q \cdot I(q)$ vs q, typically highlights the q^{-1} dependence of the data, allowing for an estimate of the persistence length of the micelles. The presence of a maximum in the bending rod plot indicates that the total contour length is greater than $2l_p$, and the relative height of the maximum to the height of the plateau or inflection gives an estimate of the number of persistence lengths per chain.[28] For solutions with added NaTosylate, the bending rod plot cannot be used to estimate l_p (Figure S4 in Supporting Information). While for zero and 0.01% added NaTosylate an inflection in the bending rod plot is observed, this inflection is not observed at higher salt concentrations, indicating that the micellar length scales are not well separated. The mesh size estimated from rheological measurements (eq 13) for 1.5% surfactant is 950 Å, which is comparable to the value of 850 Å measured for l_p by rheo-optics for 0.05% NaTosylate.

Discussion

There are several length scales that affect the rheological behavior of charged wormlike micelles, including the persistence, contour, mesh, and electrostatic screening lengths. The main goal of this work is to determine these micellar length scales systematically as a function of surfactant concentration, surfactant ratio, and salt concentration.

First consider the effect of varying added electrolyte. The SANS results indicate that intermicellar interactions decrease as sodium tosylate is added, as witnessed by the disappearance of the interaction peak in the SANS spectra (Figure 12). Note that because sodium tosylate is the common salt for both surfactants, the effects on persistence, contour, and interaction lengths are a convolution of changes in electrostatic screening, with a possible reduction in net micelle charge. Comparison with the results for added sodium chloride suggests that this effect is substantial. As sodium tosylate is added, both the zero-shear viscosity and the relaxation time decrease. This reduction in η_o and τ_R upon addition of salt is often explained by an increase in the endcap energy, E_c, which results in the presence of branched micelles.[14,15,24,25,49] In particular, the branching of micelles has been proposed to explain the reduction in η_o and τ_R upon addition of sodium tosylate to CTAB,[14] and either NaBr or potassium acetate to CTAHNC,[49] systems which contain the CTA^+ surfactant ion in the presence of hydrotropic counterions (HNC^- and Tos^-).

In order for micellar branching to occur, the formation of a 3-fold junction must be favored over endcaps. Addition of the penetrating salt to CTAT/SDBS mixed micelles decreases the persistence length (Figure 11), which itself is a measure of the one-dimensional bending modulus, $l_p = \kappa/k_BT$. This increase in flexibility may also play a role in the ability to form a three-arm branch, in which saddle-like regions are present within the junction. Therefore, the addition of sodium tosylate causes an increase in endcap energy combined with a possible decrease in the energy required to form a branch point, resulting in the formation of branched micelles. The decreases in both zero-shear viscosity and relaxation time are consistent with an increasingly branched structure as the NaTosylate concentration increases.

Next, we consider the effect of changing surfactant ratio. Anomalous rheological behavior in the form of maxima in η_o and τ_R has been previously reported without added electrolyte,[16] explained by the growth and eventual branching of micelles upon addition of SDBS to CTAT. Here, however, adding either sodium tosylate or NaCl to the system results in a monotonic decrease in η_o and τ_R. The addition of SDBS reduces the surface charge density, ν, thereby decreasing E_e (eqs 2 and 3) and initially favoring micellar growth in the absence of salt. To consider what happens to the electrostatic energy upon addition of either NaCl or NaTosylate, the Mackintosh model[20] for E_e can be extended to intermediate salt concentrations C_s by the substitution of an effective volume fraction which increases with added salt: $\bar{\phi} = \phi + 8\pi l_B r_{cs}^2 C_s$. Thus, the addition of salt increases the endcap energy and decreases E_e (eq 3), favoring micellar growth as the SDBS fraction increases. However, because the presence of salt makes endcap formation less favorable, the possibility of branching must also be considered.

Addition of SDBS increases L_o, the average distance between charges, and results in a decrease in l_p (eq 18) in the presence of both NaCl and NaTosylate (Figure 10). The increase in flexibility should favor branching due to the changes in curvature. The topological transition of cylinders to a connected network followed by phase separation is predicted to occur with decreasing spontaneous curvature,[50] and indeed phase separation occurs at higher SDBS fractions.[19] Theoretical calculations[51] suggest that for a single-component surfactant solution, as the headgroup repulsion decreases, the energy required to form a 3-fold junction decreases. The addition of SDBS to CTAT decreases the surface charge; however, the presence of either NaCl or NaTosylate also reduces the headgroup repulsion though electrostatic screening, allowing branching to occur at a lower SDBS fraction. Penetration of NaTosylate into the micelle results in an additional reduction in the headgroup repulsion, allowing branching to occur at a lower molarity than in the presence of the screening salt. The decrease in η_o and τ_R observed in this work is qualitatively consistent with the increase in branching as SDBS is added to CTAT in the presence of either salt.

(49) Narayanan, J.; Manohar, C.; Kern, F.; Lequeux, F.; Candau, S. J. *Langmuir* **1997**, *13*, 5235−5243.
(50) Tlusty, T.; Safran, S. A. *J. Phys.: Condens. Matter* **2000**, *12*, A253−A262.
(51) May, S.; Bohbot, Y.; BenShaul, A. *J. Phys. Chem. B* **1997**, *101*, 8648−8657.

Finally, we examine the effect of surfactant concentration. In the CTAT/SDBS system with no added electrolyte, anomalous behavior is seen in the form of maxima in η_o and τ_R as functions of surfactant concentration.[16] As salt screens the electrostatics, the rheology is expected to eventually approach that of a solution of nonionic micelles. However, adding a molarity of sodium chloride comparable to the molarity of the counterions coming from the highest surfactant concentrations examined cannot suppress the anomalous maximum in η_o with surfactant concentration, nor the anomalous *decrease* in τ_R with increasing surfactant concentration, although the zero-shear viscosities and relaxation times are lower than those in the salt-free system. In contrast, when the penetrating salt sodium tosylate is added, η_o increases monotonically with surfactant concentration, although still not in quantitative agreement with that predicted for nonionic micelles. The relaxation time, however, still *decreases* with increasing surfactant concentration, which is typical of the behavior of polyelectrolyte solutions[46] rather than nonionic micelles. It is well known that in dilute, salt-free solution, increasing polyelectrolyte concentration is accompanied by an increase in counterion concentration and, hence, increased electrostatic screening. This decrease in the Debye screening length results in a decrease in l_p (eq 18), which reduces the radius of gyration, R_g, and the longest relaxation time, τ_R. A similar mechanism should be operative for the CTAT/SDBS micellar solutions but is further complicated by changes in the breakage time and/or contour length due to changes in the ionic strength and surfactant concentration. Consequently, deviations from the scaling for nonionic micelles likely reflect indirect effects on the three length scales from changes in solution ionic strength.

As total surfactant concentration increases, τ_{break} decreases in the presence of both NaCl and NaTosylate. The scission rate constant, k_1, has previously been assumed to be the same for all wormlike micelles,[52] independent of solution chemistry. If k_1 is constant, then the decrease in breakage time could be attributed to an increase in $\bar{L}_c$ (eq 4) with surfactant concentration, consistent with the predictions of eq 1. The product $\tau_{break} \cdot \bar{L}_c$ depends on volume fraction[13] particularly in the presence of a strongly binding counterion, a result suggesting that the scission constant k_1 is in fact sensitive to the nature and concentration of counterions present. In addition, if micellar branching is important, the appropriate length in eq 4 becomes the distance between branch points rather than the contour length. The tosylate ion is present in solution as the counterion of CTAT/SDBS mixtures, so any inferences regarding the change in contour length or distance between branch points with the breakage time cannot be made unambiguously.

As surfactant concentration is increased, the persistence length increases slightly, despite the increase in electrostatic screening due to the counterions. This is presumably due to the presence of interchain interactions as revealed by the SANS spectra. The mesh size and entanglement length both decrease as C_D increases. For solutions with added NaCl, these three length scales begin to converge at surfactant concentrations greater than approximately 2.5%. This would suggest that these values at the higher surfactant concentrations should be taken with caution as the theories and models used to extract them generally assume the length scales are widely separated. The rheological parameters also undergo a transition at these higher surfactant concentrations. In particular, the zero-shear viscosity goes through a maximum at a surfactant concentration of 1.5% (in the presence of NaCl), at which point the scaling of the relaxation time with C_D changes slope. The convergence of length scales and the changes in rheological properties all suggest that either micellar branching occurs at these higher surfactant concentrations or the micelles can no longer be considered in the semidilute regime. Branching is consistent with both the decrease in η_o and the change in slope for τ_R. As surfactant concentration continues to increase, the branched micellar network becomes saturated, and these three measured length scales (l_p, l_e, and ξ_M) become indistinguishable. The formation of a branched network is predicted[50,53,54] to be concentration dependent, and cyro-TEM results[55] further support an increased degree of branching with surfactant concentration.

Candau and Oda use the analogy to polyelectrolytes to discuss the rheological scaling of the relaxation time and zero-shear viscosity of charged wormlike micelles.[56] For reversible scission, the zero-shear viscosity and relaxation time scale as $\eta_o \propto k_1^{-1/2} \bar{L} c^{3/2}$ and $\tau_R \propto k_1^{-1/2} \bar{L}$. For highly branched micelles, the appropriate micellar length is the distance between branches, which scales as[57] $\bar{L} \propto c^{-1/2}$, resulting in an increasing viscosity but decreasing relaxation time with surfactant concentration. While the data for CTAT/SBDS micelles in the presence of added salt do not quantitatively follow these scaling laws, the qualitative trend of increasing viscosity with decreasing relaxation time further supports the conjecture of micellar branching with increasing concentration.

Although no anomalous maximum is observed in the zero-shear viscosity as a function of surfactant concentration for solutions with added NaTosylate, a similar transition in microstructure occurs at a comparable surfactant concentration. Above a C_D of approximately 1.5%, the slope of the zero-shear viscosity decreases from $\eta_o \sim C_D^{1.4\pm0.1}$ to $C_D^{0.56\pm0.05}$, and the relaxation time also undergoes a change in slope from $\tau_R \sim C_D^{-0.63\pm0.09}$ to $C_D^{-1.54\pm0.03}$. Again, this is consistent with the onset of micellar branching or entry to a different concentration regime. Note that at 1.5 wt % 97/3 surfactant concentration and 0.25 wt % NaTosylate there are no intermicellar interactions evident in the SANS spectra (Figures 12 and S4); hence the transition is not a consequence of significant electrostatic intermicellar interactions. At a C_D of 4%, the measured length scales begin to overlap, again indicating that the micellar network is becoming saturated.

Conclusions

Figure 1 shows the quantification of the four dominant length scales controlling the rheology of micellar solutions that are extracted from combination of rheology, SANS, and rheo-optics measurements. These length scales vary systematically with solution ionic strength, surfactant composition, and surfactant adsorption and provide a microstructural rationalization for the seemingly anomalous rheology observed for mixed ionic micellar solutions.

The addition of small amounts of NaCl and NaTosylate to CTAT/SDBS wormlike micelles moderates the anomalous rheological behavior observed for solutions without added salt; however, the scaling predicted for nonionic

(52) Cates, M. E. *J. Phys. Chem.* **1990**, *94*, 371−375.
(53) Bohbot, Y.; Benshaul, A.; Granek, R.; Gelbart, W. M. *J. Chem. Phys.* **1995**, *103*, 8764−8782.
(54) Drye, T. J.; Cates, M. E. *J. Chem. Phys.* **1992**, *96*, 1367−1375.
(55) Bernheim-Groswasser, A.; Wachtel, E.; Talmon, Y. *Langmuir* **2000**, *16*, 4131−4140.
(56) Candau, S. J.; Oda, R. *Colloid Surf., A* **2001**, *183*, 5−14.
(57) Khatory, A.; Lequeux, F.; Kern, F.; Candau, S. J. *Langmuir* **1993**, *9*, 1456−1464.

micelles is not observed. Rather, solutions with added sodium tosylate behave qualitatively similar to polyelectrolytes, with the zero-shear viscosity increasing while the relaxation time decreases as total surfactant concentration increases. In the case of solutions with added NaCl, this polyelectrolyte behavior is observed at low surfactant concentrations, before the onset of micellar branching likely occurs. Micellar branching is suggested because the persistence length, entanglement length, and solution mesh size, as measured through a combination of rheo-optics and rheology, converge at high surfactant concentrations in the presence of either salt.

Polyelectrolyte-like behavior is also observed in the scaling of the persistence length with solution chemistry. The persistence length scales with κ^{-2} in the presence of the hydrotropic salt NaTosylate, in agreement with the OSF theory for polyelectrolytes. The persistence length decreases as SDBS is added to CTAT in the presence of either salt, consistent with the OSF prediction for a decrease in the micellar surface charge. This combination of rheo-optics and rheology allows all relevant length scales to be measured and provides the basis for an explanation of the observed rheology.

Acknowledgment. Funding for this project was from Unilever and the Delaware Research Partnership. The authors thank Dr. Alex Lips for useful discussions. We acknowledge the support of the National Institute of Standards and Technology, U.S. Department of Commerce, in providing the neutron research facilities used in this work. This work utilized facilities supported in part by the National Science Foundation under Agreement No. DMR-9986442.

Supporting Information Available: Master rheological curves for steady and dynamic rheology, verification of the stress optic coefficient using Laun's rule, a Holtzer or "Bending Rod" plot of the SANS data, and tables containing rheological parameters and micellar length scales. This material is available free of charge via the Internet at http://pubs.acs.org.

LA020821C